

# Calcium action potentials in hair cells pattern auditory neuron activity before hearing onset

Nicolas X Tritsch<sup>1,5,6</sup>, Adrián Rodríguez-Contreras<sup>2,5,6</sup>, Tom T H Crins<sup>2,3</sup>, Han Chin Wang<sup>1</sup>, J Gerard G Borst<sup>2</sup> & Dwight E Bergles<sup>1,4</sup>

**We found rat central auditory neurons to fire action potentials in a precise sequence of mini-bursts before the age of hearing onset. This stereotyped pattern was initiated by hair cells in the cochlea, which trigger brief bursts of action potentials in auditory neurons each time they fire a Ca<sup>2+</sup> spike. By generating theta-like activity, hair cells may limit the influence of synaptic depression in developing auditory circuits and promote consolidation of synapses.**

Developing sensory systems rely on intrinsically generated electrical activity to guide the maturation of circuits required for processing sensory information<sup>1</sup>. In all of the sensory modalities examined, this spontaneous activity occurs in the form of discrete bursts of action potentials separated by long periods of quiescence<sup>1,2</sup>; however, the mechanisms by which burst firing influences diverse aspects of development are largely unknown. In mature circuits, plasticity is enabled by distinct forms of activity<sup>3,4</sup>, raising the possibility that developing circuits also initiate stereotyped patterns of activity to promote efficient induction of certain signal transduction cascades.

Altricial mammals are born deaf and do not respond to sound until the second postnatal week. Nevertheless, auditory neurons fire bursts of action potentials during the prehearing period<sup>5,6</sup> that are likely initiated in the developing cochlea. Indeed, recent studies have indicated that ATP is released spontaneously from supporting cells in the developing cochlea, which depolarizes inner hair cells (IHCs) and eventually induces trains of action potentials in spiral ganglion neurons (SGNs)<sup>7,8</sup>. To define the patterns of activity exhibited by SGNs during this period, we made extracellular recordings from SGNs in cochleae that were isolated from prehearing rats (**Supplementary Methods**). Spontaneous activity in SGNs was clustered into discrete bursts that lasted  $2.6 \pm 0.3$  s, contained  $15.8 \pm 1.8$  action potentials and occurred at a frequency of  $2.6 \pm 0.4 \text{ min}^{-1}$  ( $n = 27$ ; **Fig. 1a**). In bursts, action potentials did not occur randomly but were grouped into discrete mini-bursts of one to six action potentials (average,  $1.6 \pm 0.1$ ) that repeated every 100–300 ms (**Fig. 1b,c**), suggesting that SGNs are under the influence

of a pacemaker. This firing pattern was consistent over time and similar between SGNs; interspike interval (ISI) histograms had three peaks, one near 10 ms, one between 100 and 300 ms, and one broad peak near 10 s ( $n = 31$ ; **Fig. 1d** and **Supplementary Fig. 1**), representing the intervals separating action potentials in mini-bursts, intervals separating mini-bursts and long intervals separating bursts, respectively. Another conspicuous feature of this activity was that intervals between mini-bursts consistently decreased and then increased during each burst (**Fig. 1e**). Similar burst patterns were observed at near physiological temperature ( $n = 8$ ) and in cochleae that were acutely isolated from prehearing rats ( $n = 10$ ; **Fig. 1d,e** and **Supplementary Fig. 2**). Notably, efferent input was not required to initiate rhythmic activity in SGNs, as this discharge pattern was not altered by blocking cholinergic transmission at efferent synapses (**Supplementary Fig. 3**).

To determine the mechanisms responsible for these patterns, we made whole-cell current-clamp recordings from IHCs. Release of ATP from supporting cells periodically depolarized IHCs, which often triggered trains of Ca<sup>2+</sup> spikes with ISIs of  $361 \pm 26$  ms ( $n = 7$ ) (**Fig. 2a,b**), similar to the delay between mini-bursts in SGNs ( $356 \pm 39$  ms,  $n = 27$ ,  $P = 0.9$ , two-sample  $t$  test). Notably,

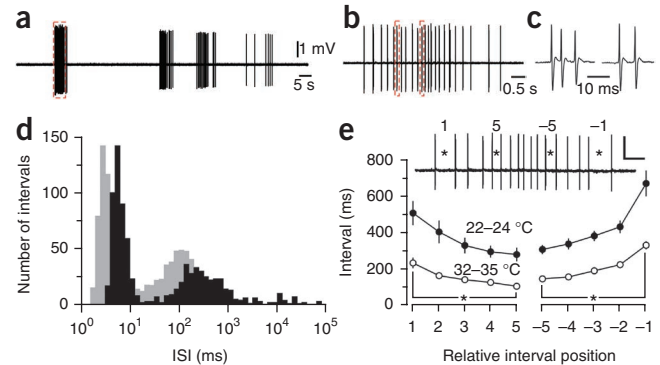


**Figure 1** SGNs fire patterned action potential bursts during the prehearing period. (a) *In vitro* extracellular recording from an SGN at 22–25 °C. (b) Detail of dashed red box in a. (c) Detail of mini-bursts highlighted in b. (d) Overlaid log-binned ISI histograms for the neuron in a (black) and a representative cell at near-physiological temperature (32–35 °C, gray). (e) Mean duration ( $\pm$  s.e.m.) of intervals separating mini-bursts as a function of their relative position in a burst for recordings performed at 22–24 °C ( $n = 302$  bursts in 23 cochleae) and 32–35 °C ( $n = 191$  bursts in 8 cochleae). Inset, example of relative mini-burst interval position at the beginning (1 and 5) and end (-1 and -5) of a spontaneous burst. Scale bars represent 0.5 mV and 0.4 s. \* $P < 0.001$ , paired  $t$  test. All experimental procedures used in this study were approved by the Animal Care and Use Committees at Johns Hopkins University and Erasmus MC.

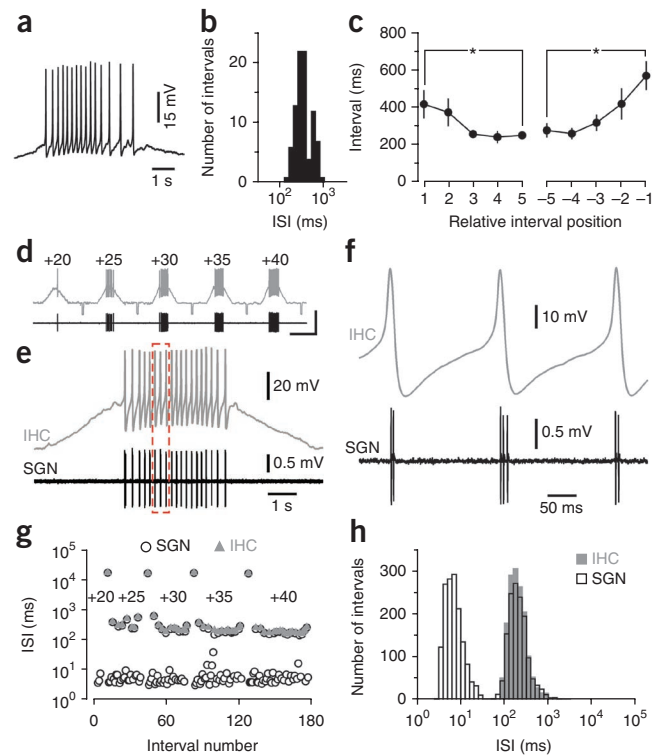
<sup>1</sup>The Solomon H. Snyder Department of Neuroscience, Johns Hopkins School of Medicine, Baltimore, Maryland, USA. <sup>2</sup>Department of Neuroscience, Erasmus MC, University Medical Center Rotterdam, Rotterdam, The Netherlands. <sup>3</sup>Department of Otorhinolaryngology-Head and Neck Surgery, University Medical Center Rotterdam, Rotterdam, The Netherlands. <sup>4</sup>Department of Otolaryngology-Head and Neck Surgery, Johns Hopkins School of Medicine, Baltimore, Maryland, USA. <sup>5</sup>Present addresses: Department of Neurobiology, Harvard Medical School, Boston, Massachusetts, USA (N.X.T.); Department of Biology, City College of New York, New York, New York, USA (A.R.-C.). <sup>6</sup>These authors contributed equally to this work. Correspondence should be addressed to D.E.B. (dbergles@jhmi.edu) or J.G.G.B. (g.borst@erasmusmc.nl).

Received 22 April; accepted 23 June; published online 1 August 2010; corrected online 15 August 2010 (details online); doi:10.1038/nn.2604

**Figure 2** IHC  $\text{Ca}^{2+}$  spikes initiate action potential mini-bursts in SGNs before hearing onset. **(a)** Spontaneous burst of  $\text{Ca}^{2+}$  spikes recorded from an IHC (22–24 °C). **(b)** Log-binned histogram of intervals separating  $\text{Ca}^{2+}$  spikes in spontaneous bursts ( $n = 7$  IHCs). **(c)** Mean duration ( $\pm$  s.e.m.) of intervals separating  $\text{Ca}^{2+}$  spikes versus relative position in a burst.  $*P < 0.05$ . **(d–g)** Simultaneous recording from an IHC (whole cell, gray) and a synaptically connected SGN (extracellular, black). **(d)** Continuous paired recording after five consecutive depolarizing current injections of increasing amplitude (20–40 pA). Small hyperpolarizing current steps ( $-10$  pA) were injected every 20 s. Scale bars represent 50 mV (top), 2 mV (bottom) and 10 s. **(e)** IHC membrane potential ( $V_{\text{rest}} = -80$  mV) in response to 40-pA injection and corresponding postsynaptic SGN firing. **(f)** Detail of dashed red box in **e**. **(g)** Plot of consecutive intervals (log scale) separating IHC  $\text{Ca}^{2+}$  spikes and SGN action potentials from the recording in **d**. **(h)** Superimposed log-binned ISI histograms for all IHC  $\text{Ca}^{2+}$  spikes and SGN action potentials pooled from 11 paired recordings. Long intervals separating current injections were excluded for clarity.

intervals between  $\text{Ca}^{2+}$  spikes progressively decreased and then increased during these events (**Fig. 2a,c**). To determine if IHC  $\text{Ca}^{2+}$  spikes were sufficient to induce SGN mini-bursts, we recorded simultaneously from IHCs and their synaptically connected SGNs (**Supplementary Fig. 4**). Slow depolarization of IHCs triggered trains of  $\text{Ca}^{2+}$  spikes in IHCs and discrete bursts of action potentials in SGNs ( $n = 11$  pairs; **Fig. 2d,e**). The vast majority of  $\text{Ca}^{2+}$  spikes (92%,  $n = 1,634$  spikes) elicited postsynaptic mini-bursts of  $2.1 \pm 0.1$  action potentials (**Fig. 2f**) separated by  $8.0 \pm 0.7$  ms ( $n = 11$ ), similar to the first peak in ISI histograms (**Fig. 1d**). Furthermore, the intervals separating IHC  $\text{Ca}^{2+}$  spikes and SGN action potential mini-bursts were indistinguishable (**Fig. 2g,h**). Thus, IHC  $\text{Ca}^{2+}$  spikes act as pacemakers to set the timing of action potentials in peripheral auditory neurons before hearing.

To determine whether activity patterns initiated in the cochlea propagate through central auditory nuclei, we made extracellular recordings *in vivo* from principal neurons in the medial nucleus of the trapezoid body (MNTB; **Supplementary Fig. 5**), a relay nucleus in the brainstem involved in sound localization<sup>9</sup>. Spontaneous activity in most MNTB neurons ( $n = 31$  of 34, 91%) in prehearing postnatal day 4–8 (P4–8) rats consisted of discrete bursts of action potentials similar to those recorded from SGNs; bursts lasted for  $2.6 \pm 0.4$  s, occurred at a frequency of  $3.2 \pm 0.3 \text{ min}^{-1}$  and contained  $16.5 \pm 2.7$  action potentials (**Fig. 3a**). Action potentials in bursts were typically clustered into



discrete mini-bursts containing  $1.5 \pm 0.1$  action potentials (**Fig. 3b,c**) and ISI histograms had distinct peaks near 10 ms, 100–300 ms and 10 s (**Fig. 3d** and **Supplementary Fig. 1**). In addition, the intervals between mini-bursts progressively decreased and then increased during each burst (**Fig. 3e**), a characteristic feature of SGN activity. This firing pattern was observed as early as P1 and was prevalent for most of the postnatal prehearing period (**Supplementary Fig. 1**). In recordings in which pre-spikes were visible ( $n = 16$  of 31), all action potentials were preceded by a prespike in 14 cells (**Fig. 3c**); in the remaining two cells, 97% of action potentials were preceded by a prespike, indicating that this activity was induced by synaptic input from the cochlear nucleus<sup>10</sup>. Moreover, spontaneously active MNTB neurons were not observed when the contralateral cochlea was removed ( $n = 6$ ; **Supplementary Fig. 6**), indicating that the patterns of activity exhibited by MNTB neurons *in vivo* are initiated in the cochlea.

To explore whether neurons in other auditory centers exhibit similar activity, we made *in vivo* extracellular recordings from the central nucleus of the inferior colliculus (CIC), a major midbrain nucleus that integrates ascending auditory information. Most recordings from CIC were composed of multiple units that exhibited highly correlated activity ( $n = 92$  of 120 recordings, 77%), consisting of bouts of action potentials lasting several seconds (**Supplementary Fig. 7**); the remaining recordings contained either a few isolated spikes or regularly discharging units. The high degree of synchrony among CIC neurons *in vivo* is consistent with ATP-mediated events in the cochlea, which initiate synchronous activity in groups of IHCs in the same region of the organ of Corti<sup>7,8</sup>. In recordings in which action potentials from individual bursting units could be discriminated ( $n = 21$ ), CIC neurons displayed firing patterns similar to those recorded from SGNs and MNTB neurons; action potentials were clustered in discrete bursts of  $8.5 \pm 1.1$  action potentials, which lasted  $1.7 \pm 0.2$  s and occurred at  $2.9 \pm 0.4 \text{ min}^{-1}$ . Although extended mini-bursts were not as frequent, ISI histograms had distinct peaks near 100–300 ms and 10 s, and intervals between mini-bursts progressively shortened and

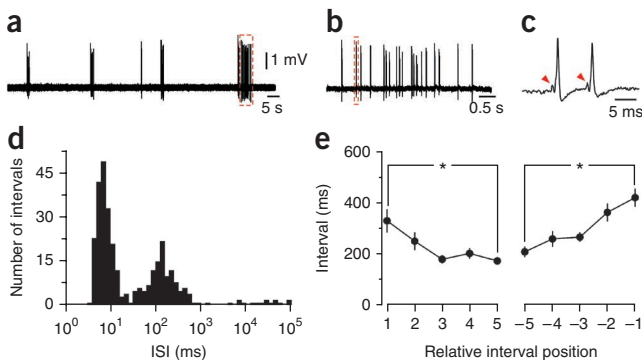


**Figure 3** MNTB neurons fire patterned action potential bursts during the prehearing period. **(a)** *In vivo* extracellular recording from a P5 MNTB neuron. **(b)** Detail of dashed red box in **a**. **(c)** Detail of the mini-burst highlighted in **b**. Arrowheads indicate prespikes. **(d)** Log-binned ISI histograms for the cell in **a**. **(e)** Mean duration ( $\pm$  s.e.m.) of mini-burst intervals in bursts ( $n = 216$  bursts in 19 units).  $*P < 0.003$ , paired *t* test.



then lengthened during each burst (**Supplementary Figs. 1 and 7**). Moreover, burst activity in CIC neurons was abolished following bilateral cochlear ablation (**Supplementary Fig. 8**), providing further evidence that the characteristic activity patterns initiated by  $\text{Ca}^{2+}$  spikes in cochlear hair cells before hearing propagate through central auditory circuits (**Supplementary Discussion**).

Pioneering studies in newborn cats have shown that auditory neurons fire rhythmically in small groups of one to several action potentials every 100–300 ms on exposure to loud sound<sup>11,12</sup>. The periodicity of this activity was influenced by the intensity, rather than the frequency, of the stimulus, in marked contrast with the sharply tuned, sustained responses observed in adults. Our results suggest that the rhythmic nature of this activity arises from generation of  $\text{Ca}^{2+}$  spikes in IHCs, which promote transmitter release from immature ribbon synapses<sup>13</sup>, but impose strict limitations on the timing of action potentials in auditory neurons.

Calyceal synapses in the auditory pathway of prehearing animals undergo pronounced synaptic depression in response to repetitive, high-frequency stimulation, which eventually prevents excitatory postsynaptic potentials from inducing action potentials<sup>9,14</sup>. Thus, clustering activity in mini-bursts is a more efficient means of propagating activity through these developing circuits. Notably, the patterns of activity that occur in the developing auditory system are similar to exogenous stimulation protocols, such as theta burst, that reliably induce long-term potentiation of excitatory synapses<sup>15</sup>. Repeated initiation of this patterned activity by subsets of IHCs at similar locations in the cochlea could therefore promote the formation and maintenance of tonotopically arranged connections in auditory centers of the brain.

*Note: Supplementary information is available on the Nature Neuroscience website.*

#### ACKNOWLEDGMENTS

This work was supported by grants from the US National Center for Research Resources (G12-RR03060) to A.R.-C., the European Union (EUSynapse, LSHM-CT-2005-019055), Heinsius Houbolt fund and SenterNovem (The Netherlands, Neuro-Bsik, BSIK 03053) to J.G.G.B., and the US National Institutes of Health (DC008860 and DC009464) to D.E.B.

#### AUTHOR CONTRIBUTIONS

N.X.T. performed the *in vitro* IHC and SGN recordings and the *in vivo* CIC recordings. A.R.-C. and T.T.H.C. performed the *in vivo* MNTB recordings. H.C.W. provided technical assistance and performed some *in vivo* CIC recordings. N.X.T., A.R.-C., J.G.G.B. and D.E.B. designed the experiments, analyzed the data and wrote the manuscript.

#### COMPETING FINANCIAL INTERESTS

The authors declare no competing financial interests.

Published online at <http://www.nature.com/natureneuroscience/>.

Reprints and permissions information is available online at <http://www.nature.com/reprintsandpermissions/>.

1. Blankenship, A.G. & Feller, M.B. *Nat. Rev. Neurosci.* **11**, 18–29 (2010).
2. Ben-Ari, Y. *Trends Neurosci.* **24**, 353–360 (2001).
3. Malenka, R.C. & Bear, M.F. *Neuron* **44**, 5–21 (2004).
4. Zhang, W. & Linden, D.J. *Nat. Rev. Neurosci.* **4**, 885–900 (2003).
5. Jones, T.A. *et al. J. Neurophysiol.* **98**, 1898–1908 (2007).
6. Sonntag, M. *et al. J. Neurosci.* **29**, 9510–9520 (2009).
7. Tritsch, N.X. *et al. Nature* **450**, 50–55 (2007).
8. Tritsch, N.X. & Bergles, D.E. *J. Neurosci.* **30**, 1539–1550 (2010).
9. von Gersdorff, H. & Borst, J.G.G. *Nat. Rev. Neurosci.* **3**, 53–64 (2002).
10. Guinan, J.J. Jr. & Li, R.Y. *Hear. Res.* **49**, 321–334 (1990).
11. Carlier, E., Abonnenc, M. & Pujol, R. *J. Physiol.* **70**, 129–138 (1975).
12. Walsh, E.J. & Romand, R. in *Development of Auditory and Vestibular Systems 2* (ed. R. Romand) 161–210 (Elsevier, Amsterdam, 1992).
13. Johnson, S.L., Marcotti, W. & Kros, C.J. *J. Physiol. (Lond.)* **563**, 177–191 (2005).
14. Brenowitz, S. & Trussell, L.O. *J. Neurosci.* **21**, 9487–9498 (2001).
15. Larson, J., Wong, D. & Lynch, G. *Brain Res.* **368**, 347–350 (1986).